

Figure 1. Stereoscopic projection of a perspective view of the crystal structure of (tetrakis(1-pyrazolylmethyl)ethene)cobalt(II) perchlorate, drawn with 20% probability ellipsoids.

methyl)-2-butene (I), prepared according to Cope and Kagan,<sup>5</sup> at room temperature. After potassium bromide was filtered off, followed by partial evaporation of the filtrate, the product crystallized. Recrystallization from acetone afforded a 40% yield of tetrakis(1-pyrazolylmethyl)ethene (II, TPAME): mp 145 °C; NMR  $\delta$  4.93 (s, 8 H), 6.27 (t, 4 H), 7.52 (d, 4 H), 7.56 (d, 4 H).

Combining methanolic solutions of II with methanolic solutions containing molar equivalents of copper(II), cobalt(II), iron(II), or nickel(II) perchlorates produced variously intensified colors and rapid formation of colored crystals.<sup>6</sup> Warming to dissolve and adding 10–20% water, followed by cooling and/or evaporation, afforded crystals suitable for X-ray crystallography.

The crystal structure of the cobalt(II) perchlorate complex is shown in Figure 1. The copper and iron complexes have the same space group and the same structure. Because of the disorder in the crystals the individual bond lengths are somewhat inaccurate.<sup>6</sup> The ring planes are rotated only 14° from the vertical planes. The N–Co–N angles and N–Co distances show that tetrapodal geometry has been achieved. The cobalt atom is 0.18 Å from the N<sub>4</sub> plane in the direction of the bound water and is 2.4 Å from the C=C plane, compared to 2.1 Å in most metal– $\pi$ -bond complexes. This means that complexes of this type are very similar to five-coordinated metalloporphyrins such as chelated protoheme in that a weakly bound fifth ligand is present.<sup>7</sup> If electron density equal to that provided by the porphyrin dianion can be supplied, such complexes might resemble metalloporphyrins. We can use a number of heterocycles to investigate both geometry and electron density. For example, tetrapodal ligands using two imidazolide and two imidazole groups should form complexes resembling metalloporphyrins.

An additional attribute of this class of ligands is the juxtaposition of the double bond. We are curious to see how the metal– $\pi$ -bond distance varies with the type and oxidation state of the metal and how these changes affect the property of the double bond. We conjecture that, using the proper CH<sub>2</sub>–C–N angle and the appropriate metal, we will be able to vary this interaction from one in which the  $\pi$  bond merely protects one coordination site to one in which the alkene–metal complex is very strong. It is possible that such a  $\pi$ -bond is a perfectly good fifth ligand for pentadentate systems. In the present case the distance from the center of the alkene to the cobalt indicates only weak interaction with the metal. It would be interesting to study the effects of altering the electron

density at the metal on its interaction with the  $\pi$ -bond.

The facile synthesis of this class of ligands through I or analogues of I containing other leaving groups, the ease of elaboration, and the ready formation and crystallization of the metal complexes make this new class of ligands attractive for transition-metal chemistry in general and biomimetic chemistry in particular.<sup>7,8</sup>

**Acknowledgment.** We wish to thank the National Institutes of Health (Grant PHS GM 39972-03) and Fogarty Fellowship (Grant 1 F06 TWO1481-01) for support, Professors Hans Freeman and Robert Armstrong of the Inorganic Chemistry Department, University of Sydney, for their hospitality during the time this work began, and Dr. Rajkumar Chadha for the crystal structures.

**Supplementary Material Available:** Tables of atomic coordinates and equivalent isotropic thermal parameters, bond distances and bond angles, anisotropic thermal parameters, and hydrogen atom coordinates and figures showing a perspective view of the structure and the unit cell packing diagram (6 pages); a table of observed and calculated structure factors (5 pages). Ordering information is given on any current masthead page.

- (8) Iron(III) perchlorate forms a crystalline complex with II. This complex is a catalyst for epoxidation of cyclohexene using pentafluoriodosylbenzene as oxidant.  
 (9) University of California, San Diego.  
 (10) University of San Diego.

Department of Chemistry, 0506,  
 University of California, San Diego,  
 9500 Gilman Drive,  
 La Jolla, California 92093-0506,  
 and Department of Chemistry,  
 University of San Diego,  
 San Diego, California 92110-2492

Teddy G. Traylor<sup>\*,9</sup>  
 Patricia S. Traylor<sup>10</sup>  
 Ben Yao Liu<sup>9</sup>

Received June 21, 1991

### A Remarkable Hypoelectronic Indium Cluster in K<sub>8</sub>In<sub>11</sub>

We have discovered that the unprecedented, electron-poor "naked" cluster anion In<sub>11</sub><sup>7-</sup> exists in the binary phase K<sub>8</sub>In<sub>11</sub>, with the added feature that one electron per formula unit is apparently delocalized in a conduction band. This result provides the first homoatomic indium cluster and evidently the first example of a

(5) Cope, A. C.; Kagan, F. J. *Am. Chem. Soc.* 1958, 80, 5499.

(6) See supplementary material paragraph at end of paper.

(7) Traylor, T. G.; Chang, C. K.; Geibel, J.; Berzinis, A.; Mincey, T.; Cannon, J. J. *Am. Chem. Soc.* 1979, 101, 6716.

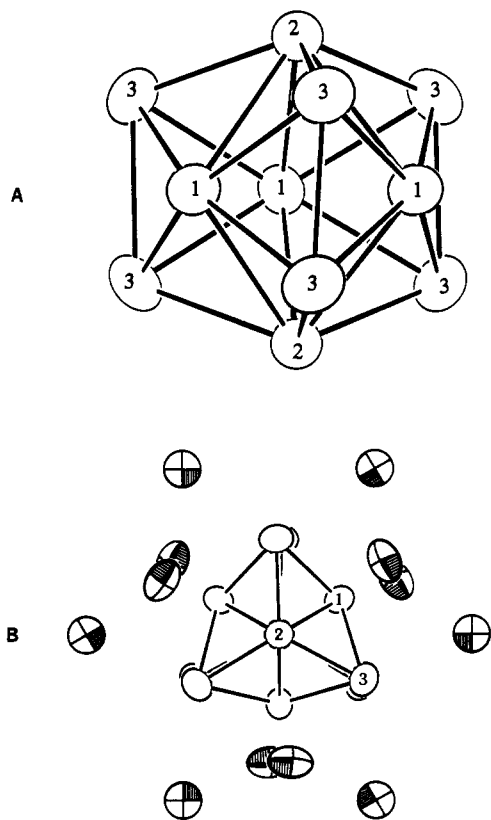


**Figure 1.** Two views of the indium cluster in  $K_8In_{11}$  (95% probability ellipsoids): A, view showing the atom-numbering system, with the 3-fold axis vertical; B, view along the  $C_3$  axis (infinite view distance) with the surrounding potassium atoms (shaded). The K2 atoms in the outer ring lie in the plane of the clusters.

stable unit well below the  $2n + 2$  skeletal minimum described by Wade's rules, in this case  $2n - 4$ . The published K-In phase diagram,<sup>1</sup> based largely on thermal analysis, shows only  $KIn_4$  ( $BaAl_4$ -type) plus an unknown phase near 36 atom % K that was first assigned as  $K_5In_8$ <sup>2</sup> and then  $K_{22}In_{39}$  (or  $K_7In_{13}$ )<sup>1</sup> on the basis of a supposedly analogous sodium-gallium phase.<sup>3</sup> Fusion of the two elements with  $\sim 40$  atom % K proportions at 530 °C followed by equilibration of the solid mixture for 2–3 days each at 400 and 300 °C readily provides the corresponding high yield of the platelike, brittle, dark gray  $K_8In_{11}$  (42.1 atom % K). Single-crystal studies<sup>4,5</sup> reveal a new type of polyhedron, the compressed pentacapped trigonal prism shown in two views in Figure 1. Atom parameters and a listing of distances and angles are included in the supplementary material.

The In-In separations range between 2.963 (1) Å (In1–In3) and 3.097 (2) Å (In3–In3) except for the slightly longer 3.284 (1) Å distance between the two types of capping atoms, In1–In2. These values compare reasonably with 2.884 Å for the single-bond distance,<sup>6</sup> 2.89–3.17 Å within the octahedra in  $Cs_2In_3$ ,<sup>7</sup> and 2.990

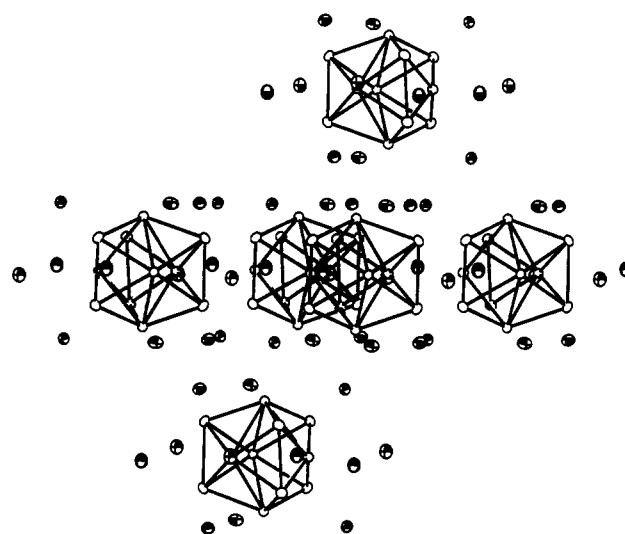


**Figure 2.** Rhombohedral stacking of cluster and potassium layers in  $K_8In_{11}$ . Half of the hexagonal cell along  $\bar{c}$  (vertical) is shown.

Å in  $Li_3In_2$  (three-bonded nets).<sup>8</sup> As shown in Figure 2, layers of indium polyhedra lying on 3-fold axes are rhombohedrally stacked along the 50.8 Å  $c$  axis, with K2 layers within and double K1 layers between the cluster layers. Potassium caps faces of the indium polyhedron at both ends (K1) and around the waist (K2), as can be seen in Figure 1B. The 3.1° torsional twist of the trigonal prism, which lowers the symmetry from  $D_{3h}$  to  $D_3$ , can be correlated with packing effects between the large clusters and the potassium layers. The shortest intercluster In–In separation is 5.260 Å.

The new polyhedron's nearest relative appears to be the ideal (but unknown) pentacapped trigonal prism from which the new cluster is generated by a sizable compression along the 3-fold axis. The triangular ends of the In3 trigonal prism are greatly expanded in the process (to 5.00 Å), but six new intercap (In1–In2) interactions at 3.28 Å are gained. The more compact result is sort of a deltahedron if we tolerate the "creases" formed by the triangles that share In1–In2 edges, which have a dihedral angle of 21.90° lying outside the cluster.<sup>9</sup> The 19 electrons available for In p-orbital bonding (assuming complete transfer from potassium) and the unlikely (but not impossible, judging from  $Sn_9$ <sup>3–10</sup>) prospect of a paramagnetic cluster prompted additional studies. The diamagnetic susceptibilities of two  $K_8In_{11}$  samples,  $-(4-5) \times 10^{-4}$  emu/mol at room temperature, decrease in magnitude by only  $\sim 10\%$  on cooling to 25 K. Corrections of  $3.1 \times 10^{-4}$  emu/mol for the ion cores and  $3.0 \times 10^{-4}$  emu/mol estimated for the Larmor precession contribution of nine electron pairs in cluster orbitals<sup>11</sup> give a net of  $+(1-2) \times 10^{-4}$  emu/mol, appropriate for a small Pauli paramagnetism. Extended-Hückel MO calculation results (below) place the last electron roughly 1.2 eV above the plausible HOMO. An alternative to this improbable result in the solid state is for the Fermi energy to fall within that gap, the last electron being delocalized over the crystal. Resistivities of two ground samples measured by the electrodeless "Q" method<sup>12</sup> over the range

(1) Pelton, A. D.; Larose, S. *Bull. Alloy Phase Diagr.* **1990**, *11*, 232.

(2) Thümmel, R.; Klemm, W. *Z. Anorg. Allg. Chem.* **1970**, *376*, 44.

(3) (a) Ling, R. G.; Belin, C. *Acta Crystallogr.* **1982**, *B38*, 1101. (b) Frank-Cordier, U.; Cordier, G.; Schäfer, H. *Z. Naturforsch.* **1982**, *37B*, 119, 127.

(4) The structure was solved by direct methods following data collection at 23 °C on a Rigaku AFC6R instrument with monochromatized Mo  $K\alpha$  radiation. Crystal data:  $R\bar{3}c$  (No. 167),  $Z = 6$ ,  $a = 10.006$  (1) Å,  $c = 50.839$  (7) Å (hexagonal setting, from Guinier powder data),  $R(F)$ ,  $R_w = 3.3$ , 3.6% for 607 independent observed reflections ( $2\theta < 50^\circ$ ) and 31 variables and with adsorption ( $\mu = 94.6$  cm<sup>-1</sup>) corrected by DIFABS (Walker, N.; Stuart, D. *Acta Crystallogr.* **1983**, *A39*, 158) ( $0.491 < \text{transm} < 1.000$ ). All lattice sites are fully occupied.

(5) After our investigations were complete, a very brief report of the same structure (with  $In_{11}^{8-}$ ) appeared, without comment or discussion: Blase, W.; Cordier, G.; Somer, M. *Z. Kristallogr.* **1991**, *194*, 150.

(6) Pauling, L.; Kamb, B. *Proc. Natl. Acad. Sci. U.S.A.* **1986**, *83*, 3569.

(7) Yatsenko, S. P.; Tschuntonow, K. A.; Orlov, A. N.; Yarmolyuk, Ya. P.; Hryn, Yu. N. *J. Less-Common Met.* **1985**, *108*, 339.

(8) Stöhr, J.; Schäfer, H. *Z. Naturforsch.* **1979**, *34B*, 653.

(9) Another cluster that is geometrically related to but chemically distant from that in  $K_8In_{11}$  is the  $Cs_{11}O_3$  unit found in several metal-rich oxide systems: Simon, A. *Struct. Bonding* **1979**, *36*, 81. Although these have the same symmetry and projection, they actually consist of three centered  $Cs_3O$  units sharing faces, and the length of the common Cs–Cs edge (equivalent to In2–In2 = 5.06 Å, Figure 1) is actually 0.4–0.6 Å less than those defining the tricapped trigonal prism; i.e., the ends of the polyhedron are concave outward. A similar construction is found in  $Ru_{11}(CO)_{23}^{3-}$ , with an axial Ru–Ru separation that is only slightly longer than that around the outside (Fumagelli, A.; Martinengo, S.; Ciani, G.; Sironi, A. *J. Chem. Soc., Chem. Commun.* **1983**, 453).

(10) Critchlow, S. C.; Corbett, J. D. *J. Am. Chem. Soc.* **1983**, *105*, 5715.

(11) Selwood, P. W. *Magnetochemistry*, 2nd ed.; Interscience Publishers: New York, 1956; pp 70, 79. The  $In^{3+}$  core value used may be too small.

(12) Shinar, J.; Dehner, B.; Beaudry, B. J.; Peterson, D. T. *Phys. Rev. B* **1988**, *37*, 2066.

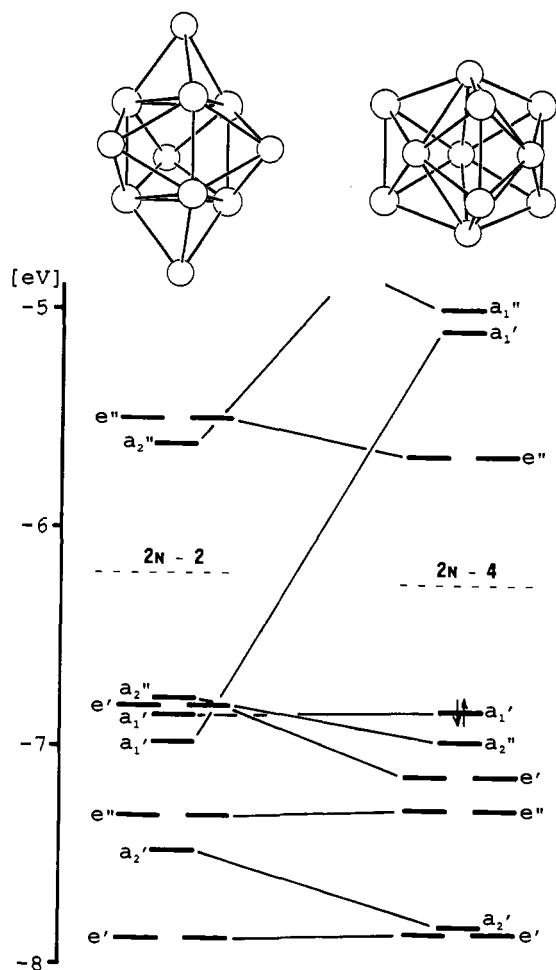


**Figure 3.** The Lower MO levels for p orbitals in  $\text{In}_{11}$  clusters with  $D_{3h}$  symmetry: left, the classical pentacapped trigonal prism ( $\bar{d} = 3.082 \text{ \AA}$ ); right, the observed axially compressed cluster with  $2n - 4$  electrons and  $\bar{d} = 3.090 \text{ \AA}$  ( $D_{3h}$  assignments). Note the increased bonding in the latter.

110–295 K indicated a metallic behavior,  $\rho_{295} \approx 600 \mu\Omega \text{ cm}$ , with a coefficient of +0.32% per degree. (It is noteworthy that liquid K–In alloys show a comparable resistivity at 475 °C,  $\sim 450 \mu\Omega \text{ cm}$ , at a large maximum near  $50 \pm 5 \text{ atom \% K}$  that has been attributed to cluster formation.<sup>13</sup> The thermodynamic excess stability of the liquid at 500 °C occurs near 35% K,<sup>14</sup> where the solid system has a network structure  $\text{K}_{22}\text{In}_{39}$ ).

We conclude that one electron per cluster is delocalized, probably over the double K1 layers (perhaps with antibonding In–In contributions) in which the shortest interlayer K–K distances, 4.05 Å, are comparable to the single-bond value, 4.00 Å.<sup>6</sup> The need for an extra potassium atom must arise from packing requirements and “solvation” of the polyanion by sufficient cations; intercalation of these layers by one halide per  $\text{K}_8\text{In}_{11}$  has not been successful. Substitution reactions with sodium have given other phases. On the other hand, the larger cation in  $\text{RbK}_7\text{In}_{11}$  disorders in half of the K2 positions with expansion of only the  $a$ – $b$  (cluster) net, while two more rubidium atoms appear to complete the K2 substitution and randomly occupied one-sixth of the K1 sites with a substantial lattice expansion in  $c$ .

The  $\text{In}_{11}^{7-}$  ion represents a new cluster-bonding configuration in an evidently unknown hypoelectronic (homoatomic) cluster regime. An analogue of the better known  $C_{2v}$  closo deltahedron with 11 vertices and 24 electrons (as for  $\text{B}_{11}\text{H}_{11}^{2-}$ ) would require an unreasonable -13 charge with  $\text{In}_{11}$ . This charge problem is alleviated for many gallium (and indium) clusters through the

formation of network structures via intercluster bonds, e.g., at all 11 vertices of the ideal  $C_{2v}$   $\text{Ga}_{11}$  unit in  $\text{K}_3\text{Ga}_{13}$ .<sup>15</sup> The only alternative mentioned in the literature appears to be ideal pentacapped trigonal prism, but this is thought to be disfavored by the presence of two vertices of order 3.<sup>16</sup> According to extended Hückel calculations,<sup>17</sup> the latter cluster exhibits a 1.2-eV HOMO–LUMO gap with only 20 p electrons ( $2n - 2$ ).<sup>18</sup> The axial compression and lateral expansion necessary to achieve the observed ( $2n - 4$ ) cluster (Figure 3) drives a single bonding  $a_1'$  orbital higher via both loss of bonding in the ends of the trigonal prism and increased antibonding In1–In2 interactions, while several occupied levels become more stable.

The general assessment of alkali-metal–indium compounds ( $\text{AB}_x$ ) as similar to gallium examples appears to be unwarranted. There are some isostructural  $\text{AB}_4$  and  $\text{AB}$  ( $\text{NaTl}$ -type) examples and common network structures for the pairs  $\text{CsGa}_3$ – $\text{CsIn}_3$ <sup>19–21</sup> and  $\text{Na}_{21}\text{Ga}_{39}$ – $\text{K}_{22}\text{In}_{39}$ .<sup>23</sup> The many evidently unique indium examples are presently under study. We also find that the unreported phase  $\text{Na}_2\text{In}$  exists and is isostructural with  $\text{Na}_2\text{Tl}$ .<sup>24</sup> This makes it formally a Zintl phase and another cluster example, as it contains isolated  $\text{In}_4$  tetrahedra with edges of 3.066 (2)–3.153 (1) Å that are isoelectronic with  $\text{Sn}_4^{4-}$  in  $\text{KSn}$ ,<sup>25</sup>  $\text{Sb}_4(\text{g})$ ,  $\text{P}_4$ , etc. Isolated gallium polyhedra are not known in any alkali-metal compound, although  $\text{Ga}_3$  and  $\text{Ga}_4$  units occur in  $\text{Ba}_8\text{Ga}_7$ .<sup>26</sup>

**Supplementary Material Available:** Tables giving data collection and refinement information, atom parameters, and distances and angles for  $\text{K}_8\text{In}_{11}$  (4 pages); a listing of observed and calculated structure factor results for the same compound (5 pages). Ordering information is given on any current masthead page.

- (15) Belin, C.; Ling, R. G. *J. Solid-State Chem.* **1983**, *48*, 40.
- (16) King, R. B.; Rouvray, D. H. *J. Am. Chem. Soc.* **1977**, *99*, 7834.
- (17) Orbital parameters and energies from: Janiak, C.; Hoffmann, R. *J. Am. Chem. Soc.* **1990**, *112*, 5924. Predominantly s-based orbitals in a cluster with the observed dimensions lie between -17.7 and -9.0 eV, while the higher block of nine bonding orbitals have on average only 2.5% In 5s population.
- (18) We were reminded that this closed-shell count can be easily derived by the addition of two axial  $\text{In}^+$  ions to the closo  $\text{In}_9^{11-}$  ( $D_{3h}$ ) ion, which adds no new bonding orbitals or p electrons (Burdett, J. K. Private communication).
- (19) Ling, R. C.; Belin, C. *Z. Anorg. Allg. Chem.* **1981**, *480*, 181.
- (20) Van Vucht, J. H. N. *J. Less-Common Met.* **1985**, *108*, 163.
- (21) Tschuntonow, K. A.; Yatsenko, S. P.; Hryn, Yu. N.; Yarmolyuk, Ya. P.; Orlov, A. N. *J. Less-Common Met.* **1984**, *99*, 15.
- (22) Reference deleted in proof.
- (23) Sevov, S. C.; Corbett, J. D. Unpublished results.
- (24) Hansen, D. A.; Smith, J. F. *Acta Crystallogr.* **1967**, *22*, 836.
- (25) Hewaldy, I. F.; Busmann, E.; Klemm, W. *Z. Anorg. Allg. Chem.* **1964**, *328*, 283.
- (26) Fornasini, M. L. *Acta Crystallogr.* **1983**, *C39*, 943.
- (27) Ames Laboratory—DOE is operated for the U.S. Department of Energy by Iowa State University under Contract No. W-7405-Eng-82. This research was supported by the Office of Basic Energy Sciences, Materials Sciences Division.

Ames Laboratory—DOE<sup>27</sup> and  
Department of Chemistry  
Iowa State University  
Ames, Iowa 50011

Slavi C. Sevov  
John D. Corbett\*

Received July 24, 1991

### A Model for the Substrate Adduct of Copper Nitrite Reductase and Its Conversion to a Novel Tetrahedral Copper(II) Triflate Complex

Denitrification, the dissimilatory transformation of  $\text{NO}_3^-$  and  $\text{NO}_2^-$  to gaseous nitrous oxide ( $\text{N}_2\text{O}$ ) and/or dinitrogen, is a central process in the biological nitrogen cycle responsible for depletion from soil of nitrogen necessary for plant growth and

- (13) Meijer, J. A.; Geertsma, W.; van der Lugt, W. *J. Phys. F: Met. Phys.* **1985**, *15*, 899.
- (14) Takenaka, T.; Petric, A.; Saboungi, M.-L. *J. Phys.: Condens. Matter* **1991**, *3*, 1603.